Chemical and Biological Technologies in Agriculture

RESEARCH

Open Access

Prenylated flavonoids isolated from the twigs of *Artocarpus champeden* as potential activators for tobacco powdery mildew and their mode of actions

Qiu-Fen Hu[1], Sui Yao[1], Yue-Yu Ma[1], Rui-Feng Xiong[1], Guang-Hui Kong[2], Yu-Ping Wu[2], Gao-Kun Zhao[2], Miao Dong[1], Wei-Guang Wang[1], Min Zhou[1*] and Yin-Ke Li[1*]

Abstract

Background *Golovinomyces cichoracearum* (DC.) is the main pathogen for tobacco powdery mildew fungus disease. Its outbreaks often result in severe harvest losses for the yield and quality of tobacco. *Artocarpus champeden* is rich in prenylated flavonoids, which are important for the plant's defensive strategies. With the aim of continuously exploring bioactive natural metabolites for agricultural chemicals, the chemical investigations on the twigs of *A. champeden* were carried out.

Results Six new (**1**–**6**) and five known (**7**–**11**) prenylated flavonoids were isolated. Compound **1** is the first example of flavone whose prenylated side-chain is converted into an unusual 1*H*-pyrrol-2-yl functional group. Compounds **2** and **3** are rare flavones bearing a 4-methylfuran-2-yl moiety. The frameworks of the above three flavones are reported in natural products for the first time. Interestingly, compound **1** showed high anti-*G. cichoracearum* activity with an inhibition rate of 88.3% ± 6.2. This rate is higher than that of the positive control (with an inhibition rate of 81.5% ± 6.3) compared to the negative control, compounds **2**–**11** also showed potential activities with inhibition rates in the range of 50.9%–72.0%. In addition, the mechanistic studies on **1** revealed that it has a potent direct effect on conidiospores of *G. cichoracearum* and induces systemic acquired resistance for tobacco plants, which may be the reasons for its significant effects against *G. cichoracearum*.

Conclusions Powdery mildew is a fungal disease harmful to tobacco. Flavonoids have been identified as the sources of promising antifungal agents. For prenylated flavonoids, the combination of a flavonoid skeleton with prenylated side-chain can give the resultant more potential for biological activities. The successful isolation and structure identification of the above prenylated flavonoids provide new materials for the screening of powdery mildew inhibitors, and also contribute to the improved utilization of *A. champeden*.

Keywords *A. champeden*, Prenylated flavonoids, *G. cichoracearum*, Antifungal activity, Tobacco powdery mildew

*Correspondence:
Min Zhou
zhouminynun@163.com
Yin-Ke Li
linkli609@163.com
Full list of author information is available at the end of the article

Graphical Abstract

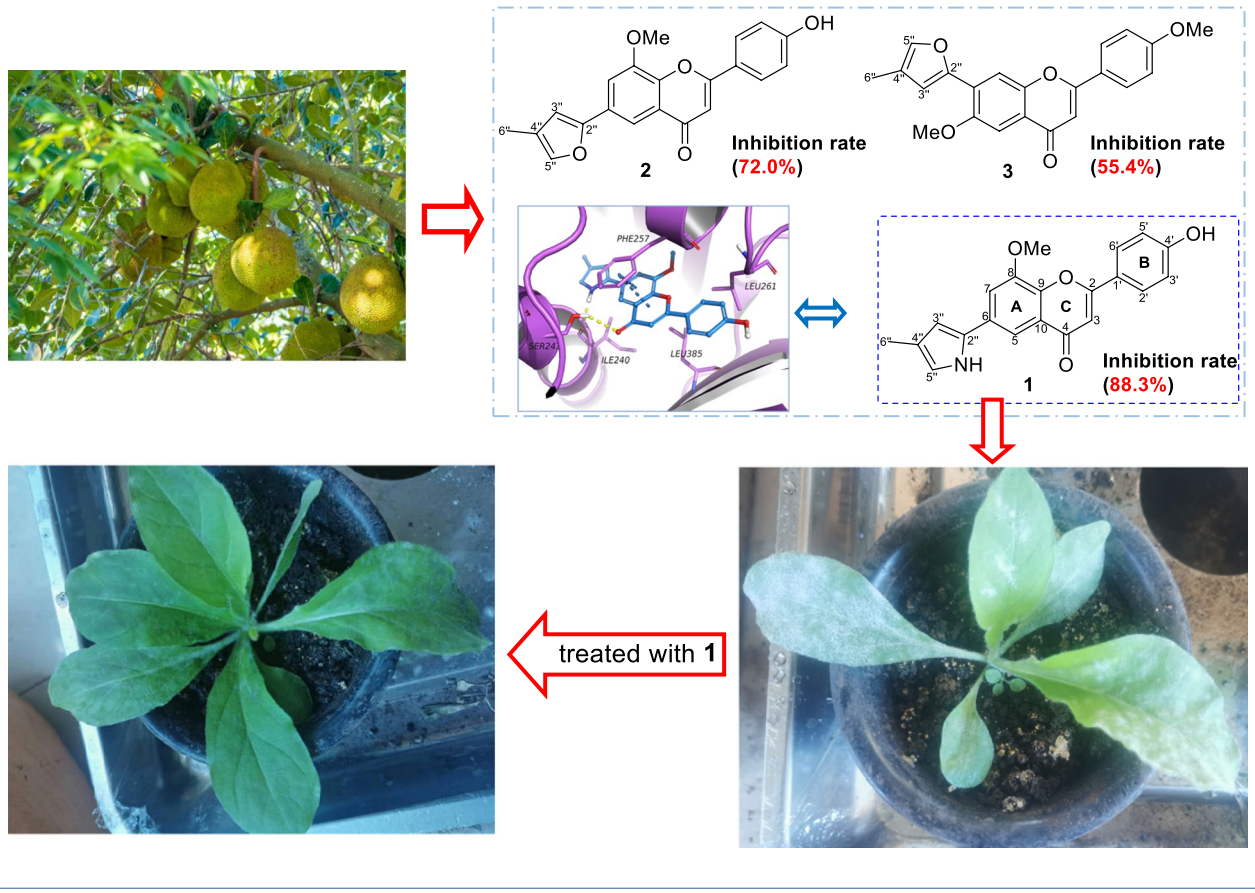

Background

Fungal diseases have harmful effects on the growth and yield of crops. Fungal pathogens attacking can cause serious losses to various crops worldwide. For main crops, their quality and yield will be notably affected once they are infected by pathogenic fungi [1, 2]. Among the most plant pathogenic fungi, *Golovinomyces cichoracearum* (DC.) is the main pathogen for powdery mildew disease, and can attack a wide range of hosts, such as tobacco, pepper, tomato, eggplant, grape, sunflower, and some melon crops [3–5]. Especially for tobacco, the powdery mildew outbreaks often result in the losses by reducing the yield and quality of tobacco leaves [6].

In agriculture, breeding resistant varieties [7, 8], inducing plants resistances [9, 10], improving cultivation [11, 12], biological control [13, 14], chemical pesticides [15, 16], and the like, are the main methods to prevent powdery mildew diseases. As compared with synthetic antifungal chemicals, natural products are highly promising prevention strategies due to their low toxicity with no residual effects [17, 18]. Therefore, they have attracted increasing attention from plant protection scholars, and also led more and more biological companies to commit to developing natural products into new pesticides [19, 20]. Among the numerous of natural products, flavonoids are associated with a group of metabolites with polyphenolic structures which are broadly found in plants. They have undertaken a variety of biological processes [21, 22], and also potentially involved in plant resistances to biotic stresses, such as protections against microbes, insects, and virus [23]. Therefore, flavonoids have been identified as promising antifungal agents [24–26].

Artocarpus champeden is a tropical fruit in the Moraceae family, which is native to India, and widely distributed in Southwest Asia. This plant has significant economic values for its fruits, woods, and folk medicine functions [27]. Previous investigations have revealed that *A. champeden* is rich in prenylated flavonoids [28–31]. Prenylated flavonoids are the combination of a flavonoid skeleton with a prenylated side-chain, and this combination can give the resultant more potential for biological activities [25]. The vertical zone climates and extensive sunlight environments provide rich plant diversity in

Yunnan Province, P.R. China. These also give the good resources for local chemists to search bioactive natural products. Since the prenylated flavonoids have been identified as promising antifungal agents with higher efficiencies [25]. With the aim of continuously exploring bioactive natural products for agricultural chemicals, the chemical investigations on the twigs of *A. champeden* were carried out. As a result, we discovered six new (**1**–**6**), as well as five known (**7**–**11**) prenylated flavonoids. Herein, the details of isolation and structure determination for above compounds, and their activities for against tobacco powdery mildew are presented in this manuscript.

Methods

General experimental procedures

UV and IR (KBr) spectra were obtained on an UV-1900 spectrophotometer (Shimadzu, Kyoto, Japan) and a FTS185 spectrophotometer (Bio-Rad, California, USA). NMR experiments were carried out on Bruker DRX-500 NMR spectrometer (Bruker, Karlsruhe, Germany) with TMS as internal standard. ESIMS and HRESI-MS analyses were performed on a 6540 Q-TOF mass spectrometer equipped with Agilent 1290 UPLC (Agilent Technologies, Wilmington, DE, USA). Microscopic observation was examined with a fluorescence biological microscope (Olympus CX33, Tokyo, Japan). 80–100 Mesh or 200–300 mesh Silica gel (Qingdao Marine Chemical, Inc., Qingdao, China) and 75–150 μm MCI CHP20P gel (Mitsubishi Chemical Corporation, Tokyo, Japan) were used for normal column chromatography. The fractions were monitored by thin-layer chromatography (Qingdao Marine Chemical, Inc., Qingdao, China), and the spots were visualized by heating silica gel plates (approximately 120 °C) after sprayed with 5% H_2SO_4 in ethanol. Semi-preparative HPLC was performed on an Agilent 1260 preparative liquid chromatography (Agilent Technologies, Wilmington, DE, USA) using a Venusil MP C_{18} column (5 μm, 2.0 cm×25 cm, Bonna-Agela, Tianjin, China) or a Zorbax PrepHT GF C_{18} column (5 μm, 2.12 cm×25 cm, Agilent, Palo Alto, USA).

Plant material

The twigs of *Artocarpus champeden (*Lour.) Stokes, were collected from Xishuangbanna Prefecture, Yunnan Province, on August 2021. The samples were dried at 35–40 °C, and then crushed to 30–60 mesh. The crushed samples were used for extraction and isolation. The species was identified by Prof. Yuan N, and the voucher specimen of the title plant (No. Ynni-21-08-047) had been deposited in the School of Ethnic Medicine, Yunnan Minzu University.

Extraction and isolation

The crushed twigs of *A. champeden* (approximately 10.0 kg) were extracted with 70% aqueous acetone and filtered, and then the solvent was removed under reduced pressure to yield the crude extract (1.02 kg). The crude extract was partitioned between water and ethyl acetate, and then decolorized with MCI GELCHP20P. The purified extract (482 g) was separated on silica gel (80–100 mesh) column with trichloromethane/methanol gradient system (10:0, 9:1, 8:2, 7:3, 6:4, and 5:5) to afforded six fractions (A–F). Fraction A (9:1, 52.6 g) was separated by silica gel column (200–300 mesh) eluted with trichloromethane/acetone (9:1 to 2:1) to yield sub-fractions B1–B7. Sub-fraction B1 (9:1, 3.85 g) was further subjected to silica gel column (200–300 mesh), and then semi-preparative HPLC (72% methanol/water, 12 mL/min) separation to yield **2** (22.5 mg), **3** (26.4 mg), **4** (26.3 mg), **5** (21.2 mg) and **6** (20.8 mg). Sub-fraction B2 (8:2, 3.21 g) was separated by another silica gel column (200–300 mesh) and subsequently separated by semi-preparative HPLC (65% methanol/water, 12 mL/min) to give **1** (28.4 mg), **7** (18.5 mg), **8** (32.4 mg), **9** (16.4 mg), **10** (13.6 (mg), and **11** (21.2 mg).

*4′-Hydroxy-8-methoxy-6-(4-methyl-1H-pyrrol-2-yl)-flavone (**1**)* $C_{21}H_{17}NO_4$, pale-yellow powder; UV (MeOH) λ_{max} (log ε) 376 (3.72), 275 (3.93), 215 (4.26) nm; IR (KBr): ν_{max} 3418, 3360, 3049, 2987, 2842, 1668, 1616, 1549, 1457, 1362, 1254, 1170, 1062, 870 cm^{-1}; ^1H and ^{13}C NMR data (500 and 125 MHz, in $CDCl_3$), see Table 1; ESIMS *m/z* 370; HRESI-MS *m/z* 370.1053 $[M+Na]^+$ (calcd $C_{21}H_{17}NNaO_4$ for 370.1050).

*4′-Hydroxy-8-methoxy-6-(4-methylfuran-2-yl)-flavone (**2**)* $C_{21}H_{16}O_5$, pale-yellow powder; UV (MeOH) λ_{max} (log ε) 374 (3.75), 278 (3.96), 215 (4.29) nm; IR (KBr): ν_{max} 3412, 3165, 3057, 2982, 2838, 1666, 1615, 1536, 1468, 1354, 1262, 1164, 1069, 848 cm^{-1}; ^1H and ^{13}C NMR data (500 and 125 MHz, in $CDCl_3$), see Table 1; ESIMS *m/z* 371; HRESI-MS *m/z* 371.0892 $[M+Na]^+$ (calcd $C_{21}H_{16}NaO_5$ for 371.0890).

*6,4′-Dimethoxy-7-(4-methylfuran-2-yl)-flavone (**3**)* $C_{22}H_{18}O_5$, Pale-yellow powder; UV (MeOH) λ_{max} (log ε) 380 (3.74), 282 (3.91), 215 (4.22) nm; IR (KBr): ν_{max} 3152, 3063, 2979, 2832, 1669, 1617, 1542, 1464, 1359, 1270, 1161, 1072, 883 cm^{-1}; ^1H and ^{13}C NMR data (500 and 125 MHz, in $CDCl_3$), see Table 1; ESIMS *m/z* 385; HRESI-MS *m/z* 385.1049 $[M+Na]^+$ (calcd $C_{22}H_{18}NaO_5$ for 385.1046).

*4′-Hydroxy-8-methoxy-6-prenyl-flavone (**4**)* $C_{21}H_{20}O_4$, Pale-yellow powder; UV (MeOH) λ_{max} (log ε) 362 (3.70), 268 (3.85), 215 (4.16) nm; IR (KBr): ν_{max} 3392, 2928, 2835, 1668, 1644, 1605, 1583, 1435, 1322, 1265, 1143, 1046, 849 cm^{-1}; ^1H and ^{13}C NMR data (500 and 125 MHz, in $CDCl_3$), see Table 1; ESIMS *m/z* 359; HRESI-MS *m/z* 359.1262 $[M+Na]^+$ (calcd $C_{21}H_{20}NaO_4$ for 359.1254).

Table 1 ^{1}H and ^{13}C NMR data for compounds **1**–**3** ($CDCl_3$, 500 and 125 MHz)

No.	Compound 1		Compound 2		Compound 3	
	δ_C (mult.)	δ_H (mult, J, Hz)	δ_C (mult.)	δ_H (mult, J, Hz)	δ_C (mult.)	δ_H (mult, J, Hz)
2	163.5 s		163.5 s		163.3 s	
3	105.3 d	6.62 s	105.2 d	6.63 s	105.3 d	6.64 s
4	177.7 s		177.6 s		177.6 s	
5	124.4 d	7.89 (d) 1.8	123.3 d	7.84 (d) 1.6	115.8 d	7.44 s
6	129.6 s		127.5 s		152.3 s	
7	115.8 d	7.39 (d) 1.8	116.4 d	7.38 (d) 1.6	124.6 s	
8	154.8 s		154.3 s		116.9 d	7.41 s
9	146.9 s		146.7 s		151.3 s	
10	126.2 s		126.5 s		125.2 s	
1′	123.4 s		123.3 s		122.7 s	
2′,6′	129.5 d	7.54 (d) 8.8	130.3 d	7.53 (d) 8.8	129.3 d	7.65 (d) 8.8
3′,5′	116.2 d	6.68 (d) 8.8	116.2 d	6.69 (d) 8.8	115.2 d	6.86 (d) 8.8
4′	157.5 s		157.6 s		160.3 s	
2′′	132.9 s		153.4 s		153.0 s	
3′′	108.6 d	6.32 s	114.7 d	6.49 s	114.3 d	6.46 s
4′′	121.0 s		116.9 s		116.9 s	
5′′	118.8 d	6.85 s	140.4 d	7.44 s	138.5 d	7.44 s
6′′	13.2 q	1.93 s	10.2 q	1.96 s	10.3 q	1.95 s
–OMe-8	56.2 q	3.83 s	56.1 q	3.83 s		
–OMe-6					56.0 s	3.77 s
OMe-4′					55.7 q	3.80 s
Ar–OH-4′		10.22 s		10.23 s		
–NH		8.64 s				

7,4′-Dihydroxy-8-methoxy-6-prenyl-flavone (**5**) $C_{21}H_{20}O_5$, Pale-yellow powder; UV (MeOH) λ_{max} (log ε) 359 (3.73), 265 (3.82), 215 (4.13) nm; IR (KBr): ν_{max} 3402, 2933, 2840, 1665, 1648, 1607, 1580, 1432, 1326, 1269, 1148, 1042, 864 cm^{-1}; ^{1}H and ^{13}C NMR data (500 and 125 MHz, in $CDCl_3$), see Table 1; ESIMS *m/z* 375; HRESI-MS *m/z* 375.1205 $[M+Na]^+$ (calcd $C_{21}H_{20}NaO_5$ for 375.1203).

6-(2,2-Dimethyl-2H,6H-pyrano[3,2-g])-4′-hydroxy-8-methoxy-flavone (**6**) $C_{21}H_{18}O_5$, pale-yellow powder; UV (MeOH) λ_{max} (log ε) 370 (3.76), 284 (3.85), 215 (4.19) nm; IR (KBr): ν_{max} 3397, 2946, 2835, 1668, 1639, 1610, 1571, 1446, 1370, 1263, 1156, 1049, 880 cm^{-1}; ^{1}H and ^{13}C NMR data (500 and 125 MHz, in $CDCl_3$), see Table 1; ESIMS *m/z* 373; HRESI-MS *m/z* 373.1049 $[M+Na]^+$ (calcd $C_{21}H_{18}NaO_5$ for 373.1046).

Microscopic observation

The conidiospores of *G. cichoracearum* were peeled from the leaves surface using transparent tapes and then installed them on a microscope slides for observation. The slides were examined and photographed with a fluorescence biological microscope (Olympus CX33, Tokyo, Japan) at 400 (10×40) and 1600 (16×100) magnifications, respectively.

Antifungal activity assays

For antifungal activity assays, the inhibition rates for compounds were tested according to the previous literatures [10, 32]. For compounds with significant activities in inhibition rates assay, their protective and the curative effects on *G. cichoracearum* were also evaluated. The detailed procedures are listed in Additional file 1: Figure S2.

Analysis of defense enzymes activities

The activities of phenylalanine ammonia lyase (PAL), peroxidase (POD), polyphenol oxidase (PPO), superoxide dismutase (SOD), catalase (CAT), and ascorbate peroxidase (APX) were determined using enzyme assay reagent kits according to the manufacturer's instructions (Jiancheng Bioengineering Research Institute, Nanjing) and literature [33]. The *N. tabacum* cv. HD plants were used as hosts. After 24 h of infection with *G. cichoracearum*, the tobacco leaves were sprayed with 250 μg/mL of the compounds. Then, the leaves were harvested on 1, 3, 5, and 7 days, and used for the determination of the activities of above enzymes.

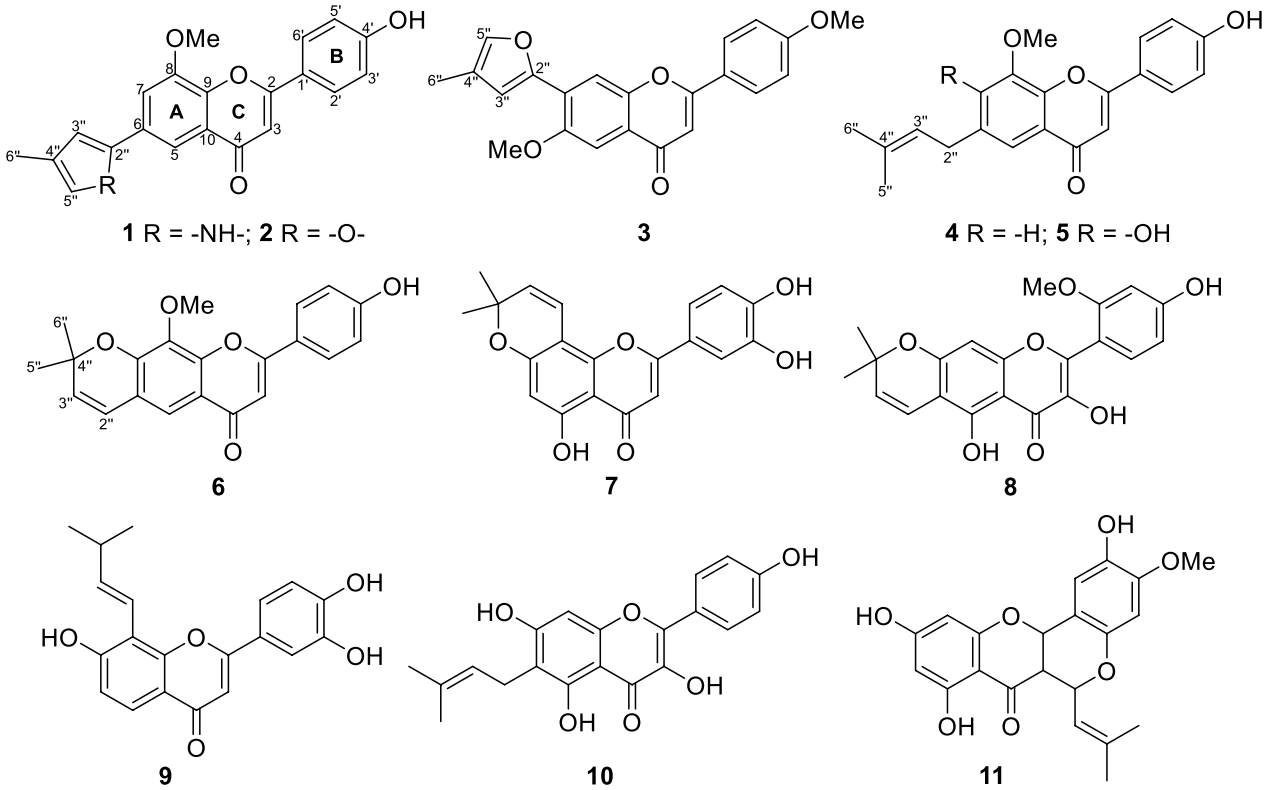

Fig. 1 Isoprenylated flavones from the twigs of *A. champeden*

Analysis of SA, JA, MDA, and CHL accumulation

The amount of salicylic acid (SA), jasmonic acid (JA), malondialdehyde (MDA), and chlorophyll (CHL) were determined by SA, JA, MDA, and CHL assay reagent kits in accordance with the manufacturer's instructions (Comin Bioengineering Institute, Suzhou, P. R. China). The *N. tabacum* cv. HD plants were infected with *G. cichoracearum*. After 24 h of infection, the plants were sprayed with 250 μg/mL of the compounds. Then the leaves were harvested on 1, 3, 5, and 7 days, and used for the determination of SA, JA, MDA, and CHL contents. The CHL contents were expressed as the plus of chlorophyll-*a* and chlorophyll-*b*.

Quantitative real-time PCR analysis of defense-related genes

The quantitative real-time PCR analysis of defense-related genes (PR-1, PR-5, PAL and Chit-1) was performed according to previous literatures [34, 35]. The materials used, detailed procedures, and the primer pairs are listed in Additional file 1: Figure S3.

Molecular docking

The molecular docking calculations were executed using AutoDock Vina software with Tubulin (*G. cichoracearum*) proteins as target. The protein sequence was got from the NCBI database (*GenBank: RKF84170.1,* https://www.ncbi.nlm.nih.gov/protein/RKF84170.1) [36]. The 3D protein structures were built by homology model using Modeller10.1, and the ligands' structures were generated by chem3D. For molecular docking calculations, the pdbqt files for the proteins and ligands were prepared according to the AutoDock protocol. All docking parameters were conserved to their default values, except the maximum number of energy evaluation (eval) and the number of genetic algorithms (GA) runs. The docking grids were made to binding sites for the receptor with a grid size of 40 Å * 40 Å * 40 Å. The grid spacing values were adjusted to 0.375 Å. Gasteiger atomic partial charges were assigned for all investigated ligands.

Results and discussion

Structure characterization of compounds 1–11

The extract obtained from the twigs of *A. champeden* was repeatedly separated by various column chromatography and preparative HPLC to afford six new (**1**–**6**), along with five known prenylated flavonoids (**7**–**11**). The structures of compounds **1**–**11** are shown in Fig. 1, and the ^{1}H and ^{13}C NMR data of **1**–**6** are listed in Tables 1

Table 2 ^{1}H and ^{13}C NMR data for compounds **4**–**6** ($CDCl_3$, 500 and 125 MHz)

No.	Compound 4		Compound 5		Compound 6	
	δ_C (mult.)	δ_H (mult, J, Hz)	δ_C (mult.)	δ_H (mult, J, Hz)	δ_C (mult.)	δ_H (mult, J, Hz)
2	163.2 s		163.4 s		162.9 s	
3	105.4 d	6.62 s	105.2 d	6.62 s	105.7 d	6.62 s
4	177.8 s		177.7 s		177.9 s	
5	123.2 d	7.89 (d) 1.8	119.0 d	7.14 s	119.6 d	6.78 s
6	133.7 s		126.9 s		120.9 s	
7	118.5 d	6.97 (d) 1.8	154.2 s		152.4 s	
8	153.5 s		146.3 s		143.6 s	
9	144.3 s		148.3 s		149.4 s	
10	125.0 s		118.0 s		120.1 s	
1′	123.5 s		123.6 s		123.3 s	
2′,6′	130.3 d	7.50 (d) 8.8	130.5 d	7.52 (d) 8.8	130.5 d	7.54 (d) 8.8
3′,5′	116.4 d	6.69 (d) 8.8	116.3 d	6.71 (d) 8.8	116.5 d	6.68 (d) 8.8
4′	157.7 s		157.6 s		157.8 s	
2′′	32.9 t	3.32 (d) 6.8	26.8 t	3.29 (d) 6.8	118.7 d	6.84 (d) 10.2
3′′	122.6 d	5.47 (t) 6.8	122.9 d	5.45 (t) 6.8	128.6 d	5.78 (d) 10.2
4′′	132.6 s		132.5 s		179.4 s	
5′′	18.4 q	1.53 s	18.3 q	1.54 s	28.6 q	1.57 s
6′′	25.3 q	1.72 s	25.5 q	1.74 s	28.6 q	1.57 s
–OMe-8	56.2 q	3.83 s	61.0 q	3.78 s		
Ar–OH-7				9.79 s		
Ar–OH-4′		10.25 s		10.24 s		10.24 s

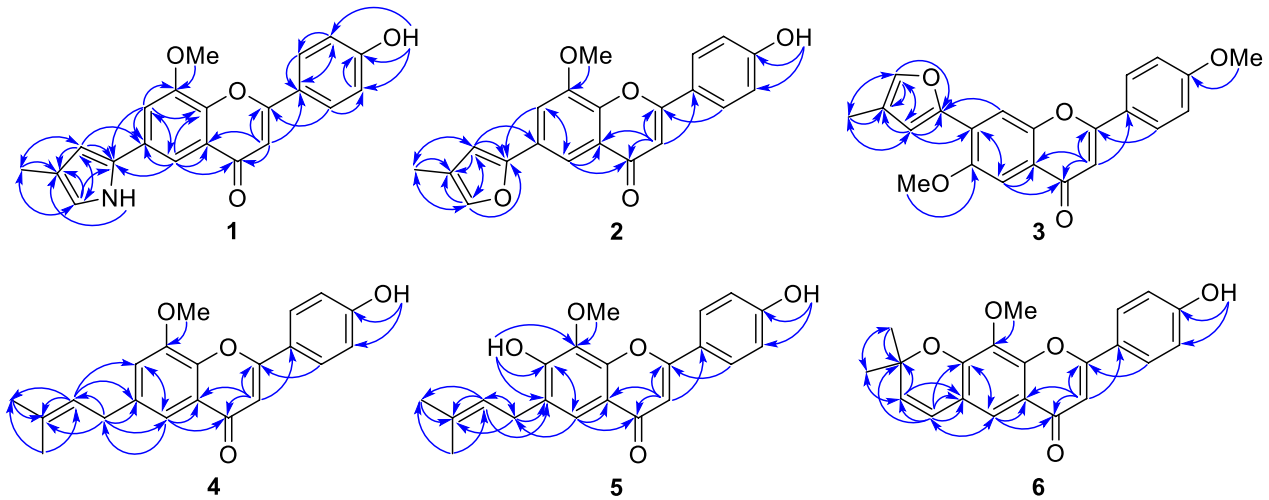

Fig. 2 The key HMBC correlations of compounds **1**–**6**

and 2. The known compounds were identified as artochamin C (**7**) [37], 2″,2″-dimethylpyran-(5″,6″:6,7)-5,4′-dihydroxy-4′-methoxy-flavonol (**8**) [38], corylifol C (**9**) [39], 6-prenyl-5,7,4′-trihydroxy-flavonol (**10**) [38], and artoindonesianin A-2 (**11**) [40], respectively, by the comparison of their NMR data with those of reported in the literatures.

To best of our knowledge, compound **1** is the first example of flavone which prenylated side-chain converted into an unusual 1*H*-pyrrol-2-yl functional group, and **2** and **3** are rare flavones bearing an unusual

4-methyl furan-2-yl moiety. The frameworks of above three new flavones are reported in natural products for the first time.

Compound **1** was obtained as a pale-yellow powder. Its molecular formula $C_{21}H_{17}NO_4$ was obtained from the quasimolecular ion peak at *m/z* 370.1053 $[M+Na]^+$ in HRESI-MS (calcd 370.1050) with 14 degrees of unsaturations. The ^1H, ^{13}C NMR, and DEPT spectral data of **1** (Table 1) displayed 21 carbon and 17 hydrogen atoms, respectively. These signals can be classified as a 1,2,3,5-tetrasubstituted benzene ring (C-5–C-10, H-5 and H-7), a 1,4-disubstitued benzene ring (C-1′–C-6′, H_2-2′,6′ and H_2-3′,5′), an *α,β*-unsaturated carbonyl (C-2–C-4, H-3), a 4-methyl-1*H*-pyrrol-2-yl moiety (C-2″–C-6″, H-3″, H-5″, H_3-6″, and –NH) [41, 42], a methoxy group (δ_C 56.2 and δ_H 3.83), and a phenolic hydroxy group (δ_H 10.22). In addition to eight degrees of unsaturations for two benzene rings, two degrees of unsaturations for *α,β*-unsaturated carbonyl, three degrees of unsaturations for pyrrole ring, the still on ring needed to support 14 degrees of unsaturations in its molecule. By further analysis of its NMR data, the existence of two oxidized aromatic quaternary carbons (C-9 and C-2) suggested that C-9 and C-2 should be linked by an oxygen atom to form a pyran ring, and **1** should be the flavone skeleton [43]. This deduction also supported by the HMBC correlations (Fig. 2) from H-3 to C-4/C-10/C-1′, from H-5 to C-4/C-9/C-10, and from H-2′ to C-2. Furthermore, the existence of 3-methylpyrrol-2-yl moiety was also supported by the HMBC correlations from H-3″ to C-2″/C-4″/C-5″/C-6″, from H-5″ to C-2″/C-3″/C-4″, from H-6″ to C-3″/C-4″/C-5″, and from –NH to C-2″/C-3″/C-4″/C-5″.

Since the flavone skeleton and the main substituents were determined, the positions of substituents can also be determined by further analyzed of its HMBC correlations (Fig. 2). The HMBC correlations from methoxy proton signal (δ_H 3.83) to C-8 indicated that the methoxy group located at C-8. The 4-methyl-pyrrol-2-yl moiety located at C-6 was supported by the HMBC correlations from H-3″ to C-6, from H-5 and H-7 to C-2″, and from –NH to C-6. Finally, the phenolic hydroxy group located at C-4′ was supported by the HMBC correlations of phenolic hydroxy proton (δ_H 10.22) with C-4′/C-3′,5′. Thus, the structure of **1** was elucidated, and given the systematic name of 4′-hydroxy-8-methoxy-6-(4-methyl-1*H*-pyrrol-2-yl)-flavone.

Compound **2** was obtained as a pale-yellow powder. It has the molecular formula $C_{21}H_{16}O_5$ from HRESI-MS (*m/z*: 371.0892 $[M+Na]^+$, calcd 371.0890). The ^1H and ^{13}C NMR spectral data of **2** were highly similar to these of **1** in C-2–C-10 and C-1′–C-6′. The obvious differences were attributed to the disappearance of 4-methyl-1*H*-pyrrol-2-yl moiety, and appearance of a 4-methylfuran-2-yl moiety (C-2″–C-6″, H-3″, H-5″, and H_3-6″) [44] in **2**. The existence of 4-methylfuran-2-yl moiety was also supported by the HMBC correlations from H-3″ to C-2″/C-4″/C-5″/C-6″, from H-5″ to C-2″/C-3″/C-4″, from H-6″ to C-3″/C-4″/C-5″. In addition, the 4-methylfuran-2-yl moiety located at C-6, the methoxy group located C-8, and the phenolic hydroxy located at C-4′ can also be confirmed by further analysis of its HMBC correlations (Fig. 2). Therefore, the structure of 4′-hydroxy-8-methoxy-6-(4-methylfuran-2-yl)-flavone (**2**) was assigned as shown.

6,4′-Dimethoxy-7-(4-methylfuran-2-yl)-flavone (**3**) is also a pale-yellow powder. It molecular formula $C_{22}H_{18}O_5$ was confirmed by HRESI-MS (*m/z* 385.1049 $[M+Na]^+$, calcd 385.1046). The ^1H and ^{13}C NMR spectral data of **3** were also highly similar to these of **2** in B and C rings. The major differences were due to the replacement of a pair of doublets [δ_H 7.84 (d) 1.6 and 7.38 (d) 1.6] to a pair singlets (δ_H 7.44 s and 7.41 s), and the hydroxy group to a methoxy group at C-4′. Moreover, the HMBC correlations (Fig. 2) from H-3″ to C-7, from H-8 to C-2″ suggested that the 4-methylfuran-2-yl moiety was located at C-7. The HMBC correlations from two methoxy protons (δ_H 3.77 and 3.80) to C-6 and C-4′ indicated that two methoxy groups were attached to C-6 and C-4′, respectively. The structure of **3** was therefore defined.

6-Prenyl-8-methoxy-4′-hydroxy-flavone (**4**) was obtained as a pale-yellow powder, and which had the molecular formula of $C_{21}H_{20}O_4$ based on the HRESI-MS data. Detailed NMR spectroscopic analyses indicated that the structural differences between **2** and **4** were resulted from the replacement of a 4-methylfuran-2-yl moiety to a prenyl group [–$CH_2CH{=}(CH_3)_2$, C-2″–C-6″, H_2-2″, H-3″, H_3-5″, and H_3-6″] [45]. Therefore, compound **4** was elucidated as 4′-hydroxy-8-methoxy-6-prenyl-flavone.

The HRESI-MS of compound **5** showed an $[M+Na]^+$ ion peak at *m/z* 375.1205, and correlated with a molecular formula of $C_{21}H_{20}O_5$. The UV, IR and NMR spectral data of **5** were highly similar to these of **4**, except that **5** contained an additional phenolic hydroxy proton (δ_H 9.79 s) and disappeared an aromatic proton on ring-A. This indicated that a hydroxy group should be substituted on the A-ring of **5**. The HMBC correlations (Fig. 2) from hydroxy proton (δ_H 9.79 s) to C-6/C-7/C-8 revealed that the hydroxy group located C-7. Thus, the structure of **5** was elucidated as a new 7-hydroxy analogue of **4**.

Compound **6** was obtained as a pale-yellow powder. Its molecular formula was deduced as $C_{21}H_{18}O_5$ by HRESI-MS $[M+Na]^+$ 373.1049 (calcd $C_{21}H_{18}NaO_5$ for 373.1046). Its spectral data were comparable to those of **5**, except that the prenyl group was converted to a

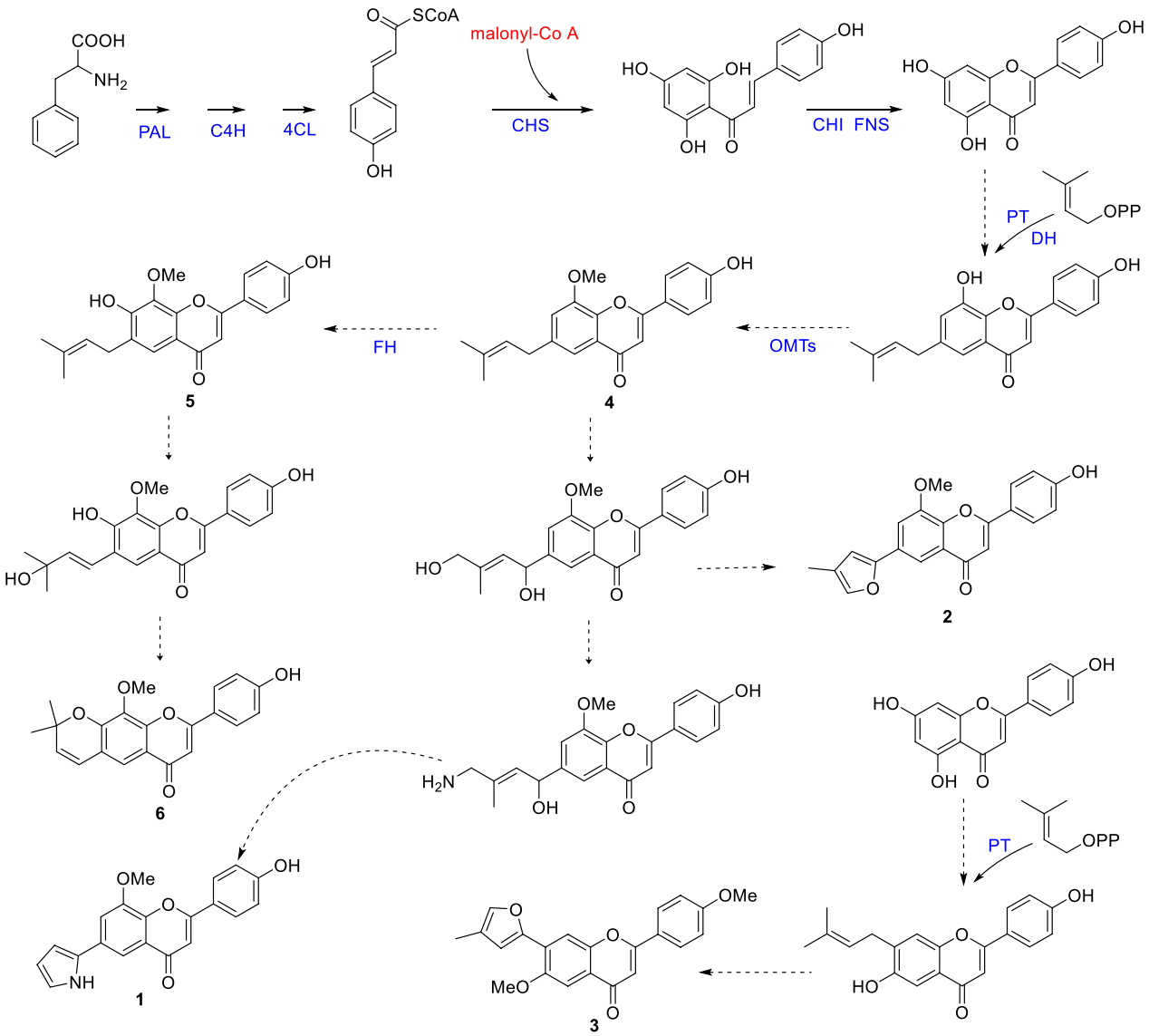

Fig. 3 The possible biogenetic pathway of compounds **1**–**6**. PAL, phenylalanine ammonia lyase; C4H, cinnamic acid 4-hydroxylase; 4CL, 4-coumarate; malonyl-Co A, malonyl-coenzyme A; CHS, chalcone synthase; CHI, chalcone isomerase; FNS, plant flavonoids synthase; PT, prenyltransferases; DH, dehydroxylase; OMTs, *O*-methyltransferases; FH, flavone hydroxylase

Table 3 The inhibition *G. cichoracearum* effects of compounds **1**–**11** on tobacco leaf

No.	Inhibition rates (%)	IC_{50} (μg/mL)	No.	Inhibition rates (%)	IC_{50} (μg/mL)
1	88.3 ± 6.2	51.5	**7**	59.9 ± 5.9	158
2	72.0 ± 5.5	106	**8**	66.7 ± 6.2	122
3	55.4 ± 5.2	147	**9**	65.1 ± 5.8	118
4	60.3 ± 5.6	159	**10**	59.2 ± 5.2	171
5	50.9 ± 5.4	195	**11**	54.1 ± 6.0	189
6	62.7 ± 6.0	153	Carbendazim	81.5 ± 6.3	70.3

gem-dimethylchromene moiety (–CH=CH–C(CH3)$_2$–O–; C-2″–C-6″; H-2″, H-3″, and H$_6$-5″,6″) [46]. This can be deducted that the prenyl should be connected to ring-A by an oxygen atom to form a *gem*-dimethylchromene ring. Moreover, two mass units less than that of **5** in MS data were also supported this deduction. Long-range correlations (Fig. 2) from H-2″ to C-5/C-6/C-7, from H-3″ to C-6, and from H-5 to C-2″ were observed. These supported that the *gem*-dimethylchromene moiety was fused at C-6 and C-7, and C-2″ was linked to ring-A. Hence, compound **6** was determined and systematically named as 6-(2,2-dimethyl-2*H*,6*H*-pyrano[3,2-*g*])-4′-hydroxy-8-methoxy-flavone.

The possible biogenetic pathway of compounds 1–6

The possible biogenetic pathway of compounds **1**–**6** was proposed as shown in Fig. 3. In plants, flavones are synthesized by the flavonoid pathway, which is part of phenylpropanoid metabolism [47]. For the biosynthesis of flavonoids, the phenylalanine was converted into coumarin-CoA through the phenylpropane pathway, then the coumarin-CoA enters the flavonoids synthesis pathway and combines with 3 molecules of malonyl-CoA to form chalcones. After this, the dihydroflavones were generated by an intramolecular cyclization reaction, and the dihydroflavones are the main precursor of other flavonoids [48]. The dihydroflavones and isoprenyl-CoA could be converted to the isoprenylflavones by isopentenylation reactions [49]. Then, compounds **1**–**6** should be derived from the isoprenylflavones by a series of oxidation, amino substitution, and epoxy reactions on pentenyl side chains, also along with the hydroxylation and methoxylation reactions on flavone nucleus.

Antifungal (*G. cichoracearum*) activity assays

Since certain of the flavonoids exhibit potential antifungal activities [50, 51], and the fungus *G. cichoracearum* (DC.) is the main pathogen of tobacco powdery mildew disease [52], Compounds **1**–**11** were tested for their anti-*G. cichoracearum* (DC.) activities.

Fig. 4 The curative effects for compound **1** on infected *N. tabacum* cv. HD. **a** Tobacco seedling infected with *G. cichoracearum*; **b**–**d** the growth of infected tobacco seedling at day 1, day 3, day 5, and day 7, after treated with 250 μg/mL of compound **1** in 0.1% Tween-20 solution; **e** control (tobacco seedling infected with *G. cichoracearum*), **f**–**h** the growth of control at day 1, day 3, day 5, and day 7, after treated with 0.1% Tween-20 solution

The antifungal activity was tested according to previous literature [10, 32], and carbendazim was used as a positive control. The results (Table 3, Additional file 1: Figure S31) revealed that **1** showed high anti-*G. cichoracearum* (DC.) activity with an inhibition rate of 88.3% ± 6.2. This rate is higher than that of the positive control (with an inhibition rate of 81.5% ± 6.3). By compared to the negative control, compounds **2**–**11** also showed notable anti-*G. cichoracearum* activities with inhibition rates in the range of 50.9%–72.0%.

The IC_{50} values of compounds **1**–**11** were also tested. The results (Table 3) revealed that **1** exhibited IC_{50} value of 51.5 μg/mL. The efficiency was higher than that of carbendazim (with IC_{50} value of 70.3 μg/mL). Compounds **2**–**11** also exhibited IC_{50} values in the range of 106–189 μg/mL. By treated *N. tabacum* cv. HD with different concentrations of **1**, the results in Additional file 1: Figure S32 revealed that the inhibition rates were increased with the increase of the concentrations of **1**, and showed a good dose–effect relationships for the infected *G. cichoracearum* on tobacco leaves.

Since the inhibition rates of **1**, **2**, **8** and **9** are higher than 70%, the protective effects of **1**, **2**, **8** and **9** on *G. cichoracearum* were also evaluated. In the protective assay, the tobacco plants were treated with the solutions of compounds (250 μg/mL). After 24 h of treatment, the *G. cichoracearum* was inoculated, and the incidences were count at day 7. The results (Additional file 1: Figure S33) revealed that **1** showed higher protective effect on the host plants with inhibition rate of 90.2% ± 6.4, and this rate is higher than that of positive control (84.2% ± 6.2). By comparing to the negative control, compounds **2**, **8** and **9** also showed good protective effects for *N. tabacum* cv. HD which infected with *G. cichoracearum*. These results indicated that the pretreatment of host plants with compounds **1**, **2**, **8** and **9** were markedly increased their resistances to *G. cichoracearum* infection.

The curative effects for **1** was also tested on *N. tabacum* cv. HD. In this experiment, compound **1** (250 μg/mL) was sprayed onto the tobacco seedlings which had been infected with powdery mildew disease, and the infected seedlings without sprayed the compound was used as a negative control. The results (Fig. 4) revealed that the powdery mildew was markedly alleviated over time after spraying with **1**. Compared to the negative control (Fig. 4a), after 24 h of spraying (Fig. 4b), the spot had obviously atrophied. After day 3 of spraying (Fig. 4c), the obvious disappearance of disease spots had been observed, and no obvious spots observed on newly grown leaves. After day 7 of spraying (Fig. 4d), the disease spots had almost completely disappeared. As compared to the negative control at the same stage (Fig. 4h), the growth of tobacco seedlings was normal and vigorous. For the tobacco seedlings without

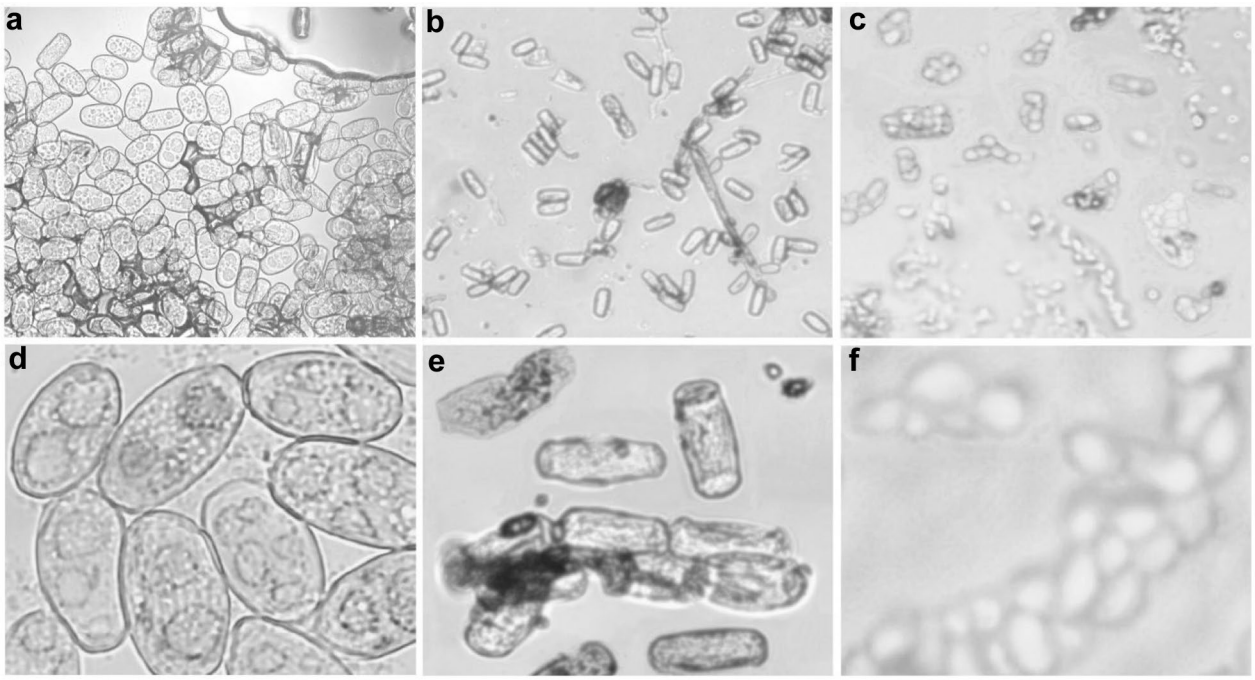

Fig. 5 The effects of compound **1** on the conidiospores of *G. cichoracearum* under light microscope. **a**–**c** 10 × 40 magnification; **d**–**f** 16 × 100 magnification. **a**, **d** Untreated with compound **1** (control); **b**, **e** after treated with 250 μg/mL of compound **1** at day 3; **c**, **f** after treated with 250 μg/mL of compound **1** at day 5

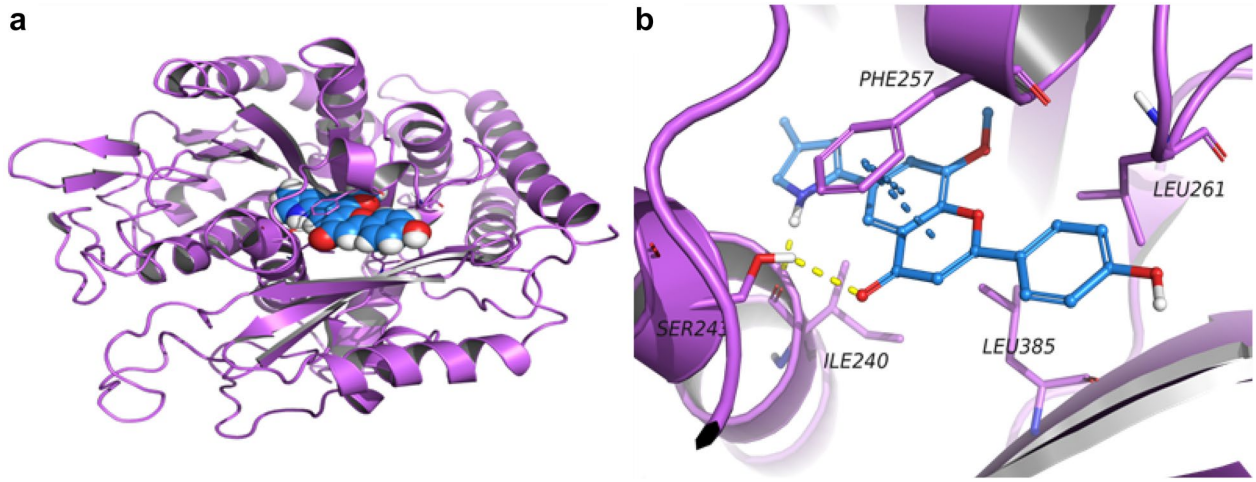

Fig. 6 The binding modes (**a** and **b**) of **1** with tubulin (*G. cichoracearum*) protein. Key residues are represented as stick models; hydrogen bonds are depicted as dotted yellow lines and pi–pi stacking interaction is depicted as dotted blue lines

spraying with **1** (Fig. 4e–h), no obvious changes were observed in powdery mildew, and the disease spots were obviously shown in the newly grown leaves. In addition, the growth of infected seedlings was also slower than that of the **1** treated group. These results indicated that **1** has a good therapeutic effect for powdery mildew disease.

The mechanism studies

Based on the above studies, **1** has the most significant activity, and the activity of **1** may involve the protective and curative effects, as well as the induction of plant resistances. Thus, the direct action of **1** on *G. cichoracearum* were observed through microscope. The results showed that when treated with **1**, the conidiospores were seriously shrunken (Fig. 5). It was clearly seen that after 24 h of spraying with **1**, most of the conidiospores were shrunken and some of the spore walls broke. In addition, the internal structures of the spores were also significantly deformed. After sprayed at day 3 (Fig. 5c), the conidiospores were further shrunken and deformed, and the normal spores were almost invisible. The above information indicted that a potent direct effect on conidiospores might be the reason for **1** against *G. cichoracearum* with significant effects.

In previous studies, the binding modes between small molecule metabolites and tubulin (*G. cichoracearum*) proteins were commonly used to evaluate the fungicides against powdery mildew activities [53, 54]. To further understanding the binding modes of **1**–**11** with tubulin proteins, the docking analysis was performed between **1**–**11** and the proteins. The docking result of **1** is shown in Fig. 6, and results of **2**–**11** are shown in Additional file 1: Figures S34 and S35.

By the docking poses analyses, **1**–**11** showed the similar docking scores to the original ligands in the crystal structure, and can strongly interact with the catalytic pocket on tubulin. This is the fundamental for anti-*G. cichoracearum* activity. For structure–activity relationships, the –C=O on nucleus of **1** can forms a hydrogen bond with Ser243, and form a π–π stacking with Phe257. The –NH on pyrrole ring can form a hydrogen bond with Ile240, while **2**–**4** lose the hydrogen bond with Ile240, and resulting in a decrease of activities. Moreover, the –OMe group on **5** has a clash with Leu261, resulting in a further decrease of activity. Compounds **6**–**10** also lost the hydrogen bond of Ile240, and this may cause the weaker activities when compared with **1**. The spatial clash with Phe257 may result in a further decrease in activity for **11**. These docking results were consistent with the above in vitro antifungal experiment.

The docking results reveal that flavonoids nucleus can interacted with Tubulin proteins, and this maybe the fundamental for direct effect on *G. cichoracearum* and play the disease resistances. In addition, the 4-methyl-1*H*-pyrrol-2-yl moiety substituted on flavone can notably increases the activity. This structure–activity relationship is proposed by our work in natural product for the first time, and it is helpful to find new antifungal activities inhibitors.

Since the activities of defense enzymes (PAL, POD, SOD, PPO, CAT, and PAX) are significantly related to plant resistances [55, 56], the activities of six enzymes in 250 μg/mL of **1** treated tobacco leaves were also analyzed. As shown in Fig. 7, the activities of six enzymes

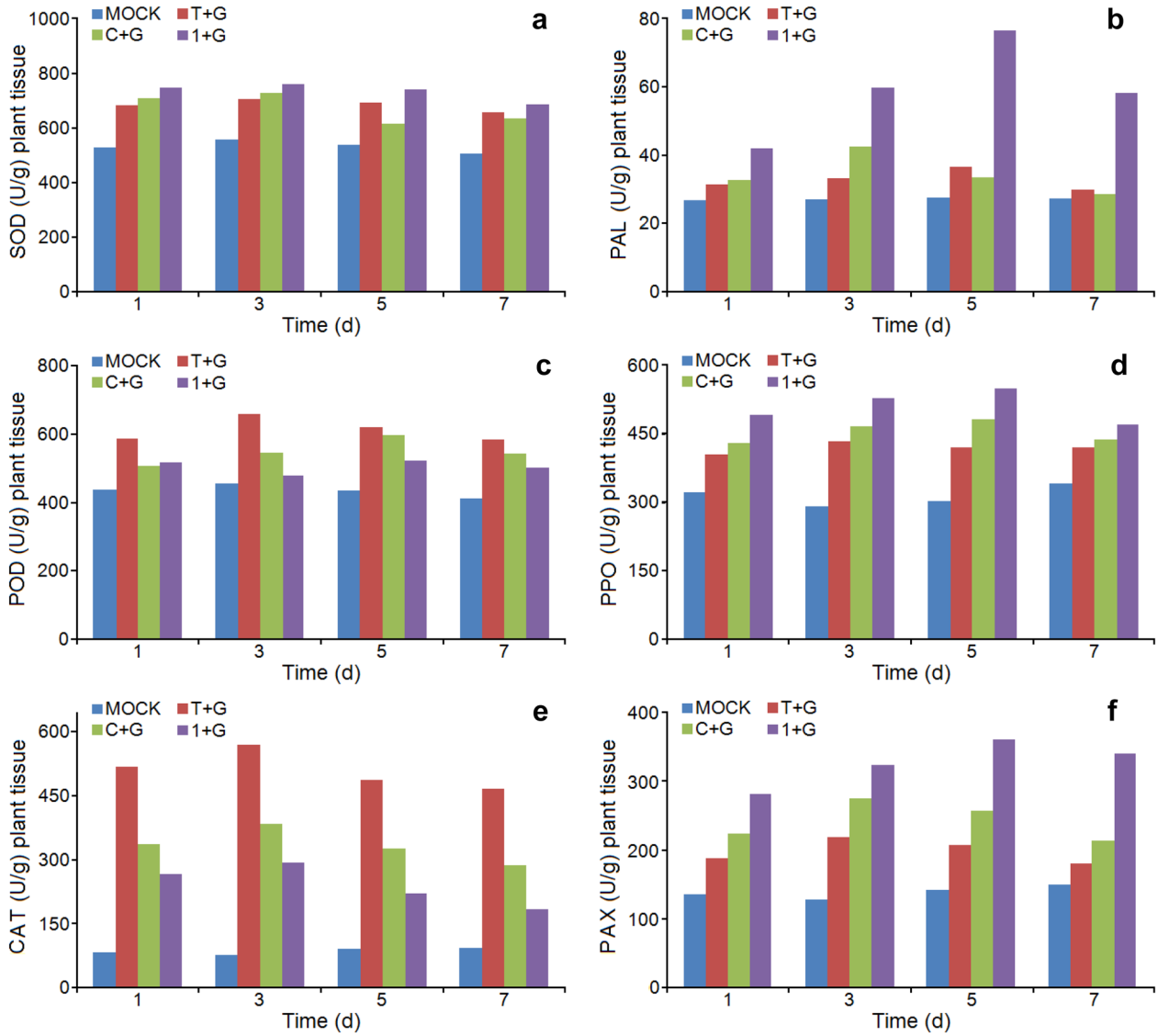

Fig. 7 The activities of SOD (**a**), PAL (**b**), POD (**c**), PPO (**d**), CTA (**e**) and PAX (**f**) in tobacco which treated with 250 μg/mL of compound **1**. Mock: healthy tobacco (negative control); T+G: *G. cichoracearum* in 0.1% of Tween-20 solution; C+G: 250 μg/mL of carbendazim in 0.1% of Tween-20 solution. **1**+G: 250 μg/mL of compound **1** in 0.1% of Tween-20 solution. All results are expressed as the average value of three determinations for all groups

for the T+G, C+G, and **1**+G groups were higher than those of in mock group. Notably, the PAL, CAT, and PAX activities had the most obvious change. In Fig. 7b, the PAL activity of **1**+G treated group in Day 5 had the highest activity; it was 2.78-fold higher than that of the mock group, 2.09-fold higher than that of the T+G group, and 2.29-fold higher than that of the C+G group. PAL is involved in the conversions of phenylpropanoids to cinnamic acid and can produce SA for defense against pathogens. The significantly induced PLA activity may be a cause of increased resistances. In Fig. 7e, the CAT activity of **1**+G treated group in day 3 had the highest activity. After fungal infection, the activity of CAT was significant increased. However, compared with the T+G group, a marked decrease in CAT activity was observed. As an important redox marker, CAT is activated to scavenge any resulting reactive oxygen species (ROS), and reduces hydrogen peroxide to oxygen and water. The results suggested that upon powdery mildew infection, the marked decreasing of CAT activity is critical for tobacco to maintain a balance ROS concentration, and therefore enhance resistance. In Fig. 7f, the APX activity of **1**+G treated group had the highest activity in Day 5. It was

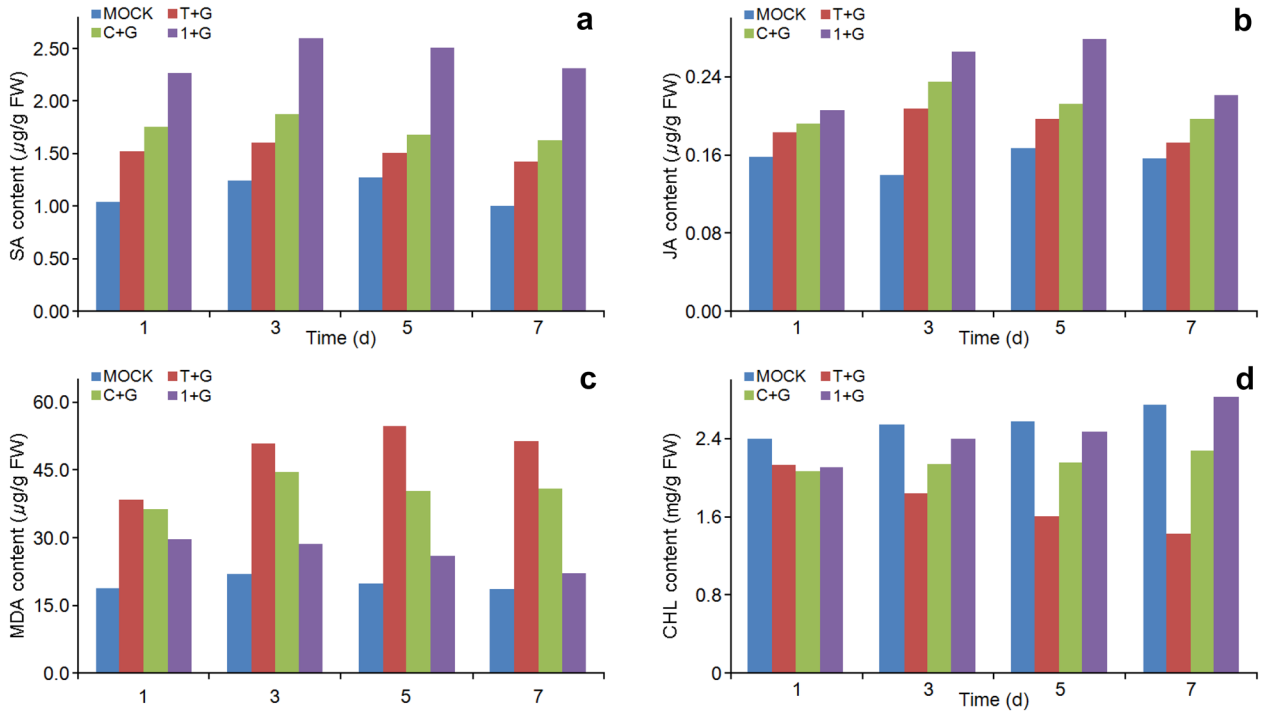

Fig. 8 The effect of compound **1** (250 μg/mL) on SA (**a**), JA (**b**), MDA (**c**), and CHL (**d**) accumulations in tobacco leaves. Mock: healthy tobacco (negative control); T+G: *G. cichoracearum* in 0.1% of Tween-20 solution; C+G: 250 μg/mL of carbendazim in 0.1% of Tween-20 solution. 1+G: 250 μg/mL of compound **1** in 0.1% of Tween-20 solution. All results are expressed as the average value of three determinations for all groups

1.74-fold higher than that of the T+G group. APX plays a very important role in physiological processes, such as plant growth and development and stress response. Especially when plants are subjected to stress, APX can quickly remove excess H_2O_2 produced in cells, and protect the plant cells from the damage caused by reactive oxygen species.

Salicylic acid (SA) and jasmonic acid (JA) are also natural plant defense hormones against pathogens [57, 58]. Since PAL can induce SA and JA, the SA and JA contents were also determined in tobacco plants. The results (Fig. 8a, b) indicated that after treated with **1**, the contents of SA and JA in tobacco plants were increased. The changes of SA content were more significant than JA. In **1**+G group, the SA contents reached a peak at day 3, and the decreased gradually from day 3 to day 7. The variation trends of **1**+G treated group were surpassed than those of in C+G and T+G treated groups. Hence, pretreated with **1** might be notably increase the SA contents and enhance plant resistance to diseases.

As a physiological indicator of cell membrane damage and an indicator of lipid peroxidation [59], the malondialdehyde (MDA) content can reflect the degrees of cell membrane lipid peroxidation and the strength of plants' response to stress conditions. When the disease-resistant substances are used to treat the infected plants, they can inhibit the increase of MDA content in the plants, thus producing a protective effect. Therefore, the MDA contents were analyzed. As can be seen from Fig. 8c, the changes of MDA content in mock group is not obvious and remains at a low level. In T+G group, the contents of MDA were significantly increased. By contrast with T+G group, the content of MDA was significantly inhibited after treated with **1**, which was also better than that of C+G group. This result showed that **1** can inhibit the increase of MDA content in tobacco leaves, thereby reducing the extent of plant damage caused by fungal infections.

In addition, chlorophylls are the major components of chloroplasts, they play an important role in photosynthesis and can provide energy for plant growth [60]. As depicted in Fig. 8d, the chlorophyll contents of tobacco leaves were decreased gradually from day **1** to day **7** after inoculated with *G. cichoracearum*. In contrast, after treated with **1**, the chlorophyll contents were increased from 2.10 to 2.82 mg/g from day 1 to

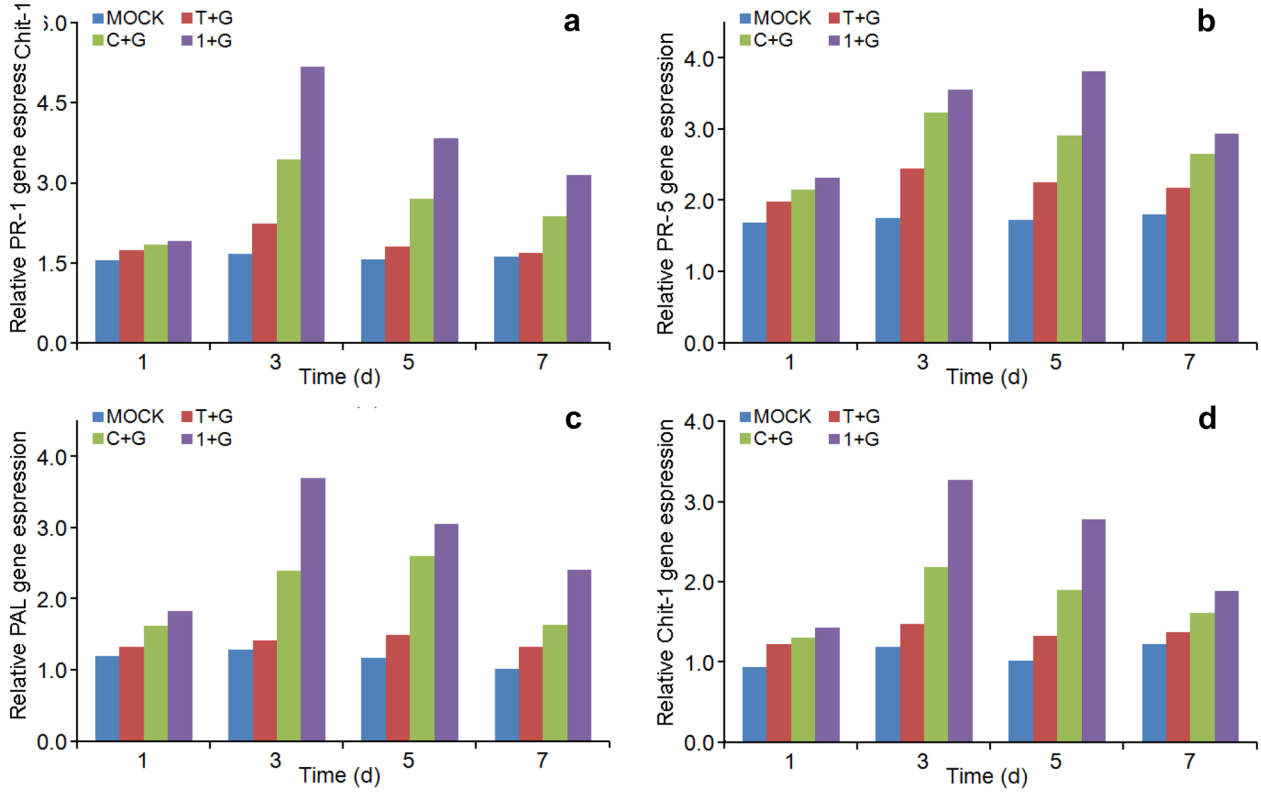

Fig. 9 The changes of the transcriptional levels for PR-1 (**a**) and PR-5 (**b**), PAL (**c**), and Chit-1 (**d**) gene in tobacco leaves treated with 250 μg/mL of compounds. Mock: healthy tobacco (negative control); T+G: *G. cichoracearum* in 0.1% of Tween-20 solution; C+G: 250 μg/mL of carbendazim in 0.1% of Tween-20 solution. 1+G: 250 μg/mL of compound **1** in 0.1% of Tween-20 solution. All results are expressed as the average value of three determinations for all groups

day 7. This indicated that treated with **1** can enhanced the photosynthetic ability of the leaves, thus improved the resistances of tobacco.

The plant resistance to fungus is closely related to the expression levels of plant defense genes. PAL gene is closely related to the formation of antibacterial functional products in the phenylpropanoid metabolism pathway, and strength of resistance to powdery mildew [61]. Chit1 gene can express chitinase, and effectively degrade the chitin components in the cell walls of higher fungi, thereby can inhibit or kill various plant pathogens [62]. PR-1 and PR-5 (the marker genes for plant disease resistances) play the functions of attack pathogens, degrade cell wall macromolecules, and degrade pathogenic toxins [63]. Therefore, their expressions of above four genes in **1**+G group were examined. The results are shown in Fig. 9. For the CK^{-} and mock groups, the changes of expression levels were not so obvious. However, in **1**+G and C+G groups, the notable up-regulation of AL, Chit1, PR-1 and PR-5 were obtained. In **1**+G group, the strongest expression levels at day 3 for PAL, Chit1, PR-1 (Fig. 9a, c, d), and at day 5 (Fig. 9b) for PR-5 were observed. These results revealed that when treated with **1**, the notable up-regulation of defense-related genes also might be the causes of enhance disease resistance.

Based on the above mechanistic studies, the mode of actions of compound **1** against *G. cichoracearum* may be involved in the potent direct effects on the conidiospores of *G. cichoracearum*; and also trigger several plant defense responses to induce the systemic acquired resistance (SAR) for the tobacco. Thus, lead to pathogen suppression and resistance to powdery mildew.

Conclusion

In this study, six new (**1**–**6**), along with five known (**7**–**11**) prenyl flavones were isolated from the twigs of *A. champeden*. Compound **1** is the first example of flavone bearing a 4-methyl-1*H*-pyrrol-2-yl functional group, and **2** and **3** are rare flavones bearing an unusual 4-methylfuran-2-yl moiety. The frameworks of above three flavones are reported in natural products by our group for the first time. Interestingly, **1** showed high activity with inhibition rate of 88.3% ± 6.2. This rate is

higher than that of positive control (with inhibition rate of 81.5% ± 6.3). Compared to the negative control, **2**–**11** also showed potential activities with inhibition rates in the range of 50.9%–72.0%. Flavonoids are potentially involved in plant resistances to biotic stresses, and they also had been identified as promising antifungal agents. However, our studies firstly reported that the prenylated flavonoids had significant effects against tobacco powdery mildew. The successful isolation and structure identification of the above prenylated flavonoids provide a new source of antifungal agents for the control of tobacco powdery mildew.

The mechanism studies also revealed that the mode of action of **1** on *G. cichoracearum* involved in the spoiling the conidiospores, and accompanied by inducing the actives of defense enzymes (PAL, CAT, and PAX), adjusting the plant hormone (SA, JA, MDA, and CHL), up-regulating the expression of defense-related genes in tobacco plant. This is also helpful for the further discovery of antifungal pesticides.

In addition, prenylated flavonoids are characterized by the presence of a prenylated side-chain, and the bioactivities of routine flavonoids can be increased by prenylation. Our study confirmed that the twigs of *A. champeden* are a rich source of prenylated flavonoids. *A. champeden* has the characteristics of rapid growth and high biological yield, which can provide the cheaper raw material sources for the extraction and utilization of prenylated flavonoids. Thus, this study also provides the beneficial proof for expanding the utilization of *A. champeden* resources.

Supplementary Information

The online version contains supplementary material available at https://doi.org/10.1186/s40538-023-00457-w.

Additional file 1: Figures S1–S5. ^{13}C, DEPT, ^{1}H, HSQC, HMBC NMR, and HRMS spectra of **1**. **Figures S5–S10.** ^{13}C, DEPT, ^{1}H, HSQC, HMBC NMR, and HRMS spectra of **2**. **Figures S11–S15.** ^{13}C, DEPT, ^{1}H, HSQC, HMBC NMR, and HRMS spectra of **3**. **Figures S16–S20.** ^{13}C, DEPT, ^{1}H, HSQC, HMBC NMR, and HRMS spectra of **4**. **Figures S21–S25.** ^{13}C, DEPT, ^{1}H, HSQC, HMBC NMR, and HRMS spectra of **5**. **Figures S26–S30.** ^{13}C, DEPT, ^{1}H, HSQC, HMBC NMR, and HRMS spectra of **6**. **Figure S31.** The inhibitory effects of **1**–**11** on *G. cichoracearum* (DC.). **Figure S32.** The dose–effect relationships of compound **1** for *G. cichoracearum*. **Figure S33.** The protective effects of compounds **1**, **2**, **8** and **9** on tobacco plant. **Figure S34.** The binding modes of compounds **2**–**7** and Tubulin (*G. cichoracearum*) protein. **Figure S35.** The binding modes of compounds **8**–**11** and Tubulin (*G. cichoracearum*) protein. **S2.** Anti-fungi activity assays. **S3.** Quantitative real-time PCR analysis of defense-related genes. **Table S1.** The primer pairs.

Acknowledgements
We appreciate the Kunming Institute of Botany, Chinese Academic Sciences, for use of the Schrodinger Suite software.

Author contributions
QH, MZ, YL, and WW designed the experiment. MD and YL prepared the samples. SY, YM, GK, RX, YW, QH, MZ, MZ, YL and GZ performed the experiments, analyzed data and wrote the paper. QH, YL, MZ, and WW reviewed and checked all the details. All authors read and approved the final manuscript.

Funding
This work was supported financially by the National Natural Science Foundation of China (32260111), the Foundation of China Tobacco Monopoly Bureau (110202101011(XJ-03)), the Foundation of Yunnan Basic Research Youth Program (2019FD119), the Candidates of the Young and Middle Aged Academic Leaders of Yunnan Province (2019HB016), and the Foundation for Key Laboratory of Yunnan Provincial Department of Education (2022HD021).

Availability of data and materials
The additional materials used for this study are available in Additional file 1.

Declarations

Ethics approval and consent to participate
Not applicable.

Consent for publication
This research has been confirmed for publication in the journal.

Competing interests
The authors have no conflicts of interest.

Author details
[1]Key Laboratory of Natural Products Synthetic Biology of Ethnic Medicinal Resources, State Ethnic Affairs Commission, Yunnan Minzu University, Kunming 650504, People's Republic of China. [2]Yunnan Academy of Tobacco Agricultural Sciences, Kunming, Yunnan 650021, People's Republic of China.

Received: 9 May 2023 Accepted: 21 August 2023
Published online: 15 September 2023

References

1. Coque J, Lvarez-Perez JM, Cobos R, Gonzalez-Garcia S, Ibaez AM, Galan AD, Calvo-Pena C. Advances in the control of phytopathogenic fungi that infect crops through their root system. Adv Appl Microbiol. 2020;111:123–70. https://doi.org/10.1016/bs.aambs.2020.01.003.
2. Peng Y, Li SJ, Yan J, Tang Y, Cheng JP, Gao AJ, Yao X, Ruan JJ, Xu BL. Research progress on phytopathogenic fungi and their role as biocontrol agents. Front Microbiol. 2021;12:670135. https://doi.org/10.3389/fmicb.2021.670135.
3. Lebeda A, Mieslerova B. Taxonomy, distribution and biology of lettuce powdery mildew (*Golovinomyces cichoracearum* sensu stricto). Plant Pathol. 2011;60(3):400–15. https://doi.org/10.1111/j.1365-3059.2010.02399.x.
4. Esawy AA, Elsharkawy MM, Omara RI, Khalifa MAF, Fadel FM, El-Naggar MM. Biological control of *golovinomyces cichoracearum*, the causal pathogen of sunflower powdery mildew. Egypt J Biol Pest Co. 2021;31(1):133. https://doi.org/10.1186/s41938-021-00479-2.
5. Sun ML, Shi CH, Huang Y, Wang HC, Li JJ, Cai LT, Luo F, Xiang LG, Wang F. Effect of disease severity on the structure and diversity of the phyllosphere microbial community in tobacco. Front Microbiol. 2023;13:1081576. https://doi.org/10.3389/fmicb.2022.1081576.
6. Shava JG, Richardson-Kageler S, Dari S, Magama F, Rukuni D. Breeding for flue-cured tobacco (*Nicotiana tabacum* L.) foliar pest and disease resistance in Zimbabwe: a review. Agric Rev. 2019;40(2):104–22. https://doi.org/10.18805/ag.R-121.
7. Tomoyuki K, Seiki S, Hisashi U, Tomoyuki T, Masao A. DNA marker development by the allele-specific detection of powdery mildew resistance loci derived from Japanese domestic tobacco cultivar 'Kokubu.' Breeding Sci. 2020;70(4):502–7. https://doi.org/10.1270/jsbbs.20011.

8. Kusch S, Ralph P. mlo-Based resistance: an apparently universal "weapon" to defeat powdery mildew disease. Mol Plant Microbe In. 2017;30(3):1943–7706. https://doi.org/10.1094/MPMI-12-16-0255-CR.
9. Kunstler A, Katay G, Gullner G, Kiraly L. Artificial elevation of glutathione contents in salicylic acid-deficient tobacco (*Nicotiana tabacum* cv. Xanthi NahG) reduces susceptibility to the powdery mildew pathogen *Euoidium longipes*. Plant Biol. 2020;22(1):70–80. https://doi.org/10.1111/plb.13030.
10. Quaglia M, Fabrizi M, Zazzerini A, Zadra C. Role of pathogen-induced volatiles in the *Nicotiana tabacum-Golovinomyces cichoracearum* interaction. Plant Physiol Biochem. 2012;52:9–20. https://doi.org/10.1016/j.plaphy.2011.11.006.
11. Villegas-Fernández AM, Amarna AA, Moral J, Rubiales D. Crop diversification to control powdery mildew in pea. Agronomy. 2021;11(4):690. https://doi.org/10.3390/agronomy11040690.
12. Chen YX, Zhang FS, Tang L, Zheng Y, Li Y, Christie P, Li L. Wheat powdery mildew and foliar N concentrations as influenced by N fertilization and belowground interactions with intercropped FABA bean. Plant Soil. 2007;291:1–13. https://doi.org/10.1007/s11104-006-9161-9.
13. Jiao R, Ahmed A, He PF, Munir S, Wu YC, Wang JW, He PB, Wang G, Yang HW, Zhao J, Lu CH, Cai YZ, He YQ. *Bacillus amyloliquefaciens* induces resistance in tobacco against powdery mildew pathogen *Erysiphe cichoracearum*. J Plant Growth Regul. 2023. https://doi.org/10.1007/s00344-023-10922-3.
14. Pan ZX, Munir S, Li YM, He PB, He PF, Wu YX, Xie Y, Fu ZW, Cai YZ, He YQ. Deciphering the Bacillus amyloliquefaciens B9601–Y2 as a potential antagonist of tobacco leaf mildew pathogen during flue-curing. Front Microbiol. 2021;12:683365. https://doi.org/10.3389/fmicb.2021.683365.
15. Gulcu B. Field efficacy of trans-cinnamic acid against powdery mildew disease, *Erysiphe corylacearum*, in hazelnut fields. Phytoparasitica. 2022;50:1091–6. https://doi.org/10.1007/s12600-022-00997-1.
16. Bhagat S, Birah A, Kumar R, Yadav MS, Chattopadhyay C. Plant disease management: prospects of pesticides of plant origin. In: Singh D, editor. Advances in Plant Biopesticides. New Delhi: Springer; 2014. https://doi.org/10.1007/978-81-322-2006-0_7.
17. Basaid KH, Chebli B, Mayad EH, Furze JN, Bouharroud R, Krier F, Barakate M, Paulitz T. Biological activities of essential oils and lipopeptides applied to control plant pests and diseases: a review. Int J Pest Manag. 2021;67(2):155–77. https://doi.org/10.1080/09670874.2019.1707327.
18. Jiménez-Reyes MF, Carrasco H, Olea A, Silva-Moreno E. Natural compounds: a sustainable alternative for controlling phytopathogens. J Chil Chem Soc. 2019;64(2):4459–65. https://doi.org/10.4067/S0717-97072019000204459.
19. Lorsbach BA, Sparks TC, Cicchillo RM, Garizi NV, Hahn DR, Meyer KG. Natural products: a strategic lead generation approach in crop protection discovery. Pest Manag Sci. 2019;75(9):2301–9. https://doi.org/10.1002/ps.5350.
20. Sparks TC, Bryant RJ. Impact of natural products on discovery of, and innovation in, crop protection compounds. Pest Manag Sci. 2022;78(2):399–408. https://doi.org/10.1002/ps.6653.
21. Warner R, Wu BS, Macpherson S, Lefsrud M. A review of strawberry photobiology and fruit flavonoids in controlled environments. Front Plant Sci. 2021;12:611893. https://doi.org/10.3389/fpls.2021.611893.
22. Ramaroson ML, Koutouan C, Helesbeux JJ, Le CV, Hamama L, Geoffriau E, Briard M. Role of phenylpropanoids and flavonoids in plant resistance to pests and diseases. Molecules. 2022;27:8371. https://doi.org/10.3390/molecules27238371.
23. Shah A, Smith DL. Flavonoids in agriculture: chemistry and roles in, biotic and abiotic stress responses, and microbial associations. Agronomy. 2020;10(8):1209. https://doi.org/10.3390/agronomy10081209.
24. Jin YS. Recent advances in natural antifungal flavonoids and their derivatives. Bioorg Med Chem Lett. 2019;29(19):126589. https://doi.org/10.1016/j.bmcl.2019.07.048.
25. Kalli S, Araya-Cloutier C, Chapman J, Sanders JW, Vincken JP. Prenylated (iso)flavonoids as antifungal agents against the food spoiler *Zygosaccharomyces parabailii*. Food Control. 2022;132:108434. https://doi.org/10.1016/j.foodcont.2021.108434.
26. Al Aboody MS, Mickymaray S. Anti-fungal efficacy and mechanisms of flavonoids. Antibiotics. 2020;9:45. https://doi.org/10.3390/antibiotics9020045.
27. de Almeida Lopes MM, de Souza KO, de Oliveira SE. Cempedak-artocarpus champeden. Exotic Fruits. 2018. https://doi.org/10.1016/B978-0-12-803138-4.00017-4.
28. Widyawaruyanti A, Subehan, Kalauni SK, Awale S, Nindatu M, Zaini NC, Syafruddin D, Setia Asih PB, Tezuka Y, Kadota S. New prenylated flavones from *Artocarpus champeden*, and their antimalarial activity in vitro. J Nat Med. 2007;61:410–3. https://doi.org/10.1007/s11418-007-0153-8.
29. Syah YM, Achmad SA, Ghisalberti EL, Hakim EH, Makmur L, Mujahidin D. Artoindonesianins Q-T, four isoprenylated flavones from *Artocarpus champeden* Spreng. (Moraceae). Phytochemistry. 2002;61(8):949–53. https://doi.org/10.1016/S0031-9422(02)00366-7.
30. Hakim EH, Fahriyati A, Kau MS, Achmad SA, Nomura T. Artoindonesianins A and B, two new prenylated flavones from the root of *Artocarpus champeden*. J Nat Prod. 1999;62(4):613–5. https://doi.org/10.1021/np980279l.
31. Taufik I, Widyawaruyanti A, Yuwono M. The metabolite fingerprints, antimalarial activities and toxicities of *Artocarpus champeden* stembark from various regions in Indonesia. Indonesian J Pharm. 2021;32(4):503–13. https://doi.org/10.22146/ijp.2384.
32. Wang HC, Yang SJ, Xu DQ, Chen XJ, Hu XD, Shang SH, Shi JX. Fungicidal activity of benzothiadiazole to *Erysiphe cichoracearum* and its safety to tobacco seedlings. Chin J Plant Prot. 2012;38(6):123–6. https://doi.org/10.3969/j.issn.0529-1542.2012.06.028.
33. Hu QF, Ma YY, Liu HY, Dai JM, Yang FX, Zhang JD, Wang J, Li XM, Liu X, Li J, Li YK, Wang WG, Zhou M, Yang GY. Antivirus isoindolinone alkaloids with rare oxocyclopenta*[f]*isoindole frameworks isolated from the stems of flue cured tobacco. Chem Biol Technol Agric. 2022;9:88. https://doi.org/10.1186/s40538-022-00339-7.
34. Yan Y, Wang D, Zhang X, Peng MY, Yan XY, Guo YS, Jia MG, Zhou J, Tang L, Hao XJ. Anti-TMV activity and effects of three prieurianin-type limonoids from *Munronia henryi*. Pestic Biochem Physiol. 2022;184:105108. https://doi.org/10.1016/j.pestbp.2022.105108.
35. Jiao R, Munir S, He PF, Yang HW, Wu YX, Wang JW, He PB, Cai YZ, Wang G, He YS. Biocontrol potential of the endophytic Bacillus amyloliquefaciens YN201732 against tobacco powdery mildew and its growth promotion. Biol Control. 2019;143:104160. https://doi.org/10.1016/j.biocontrol.2019.104160.
36. Sachse C, Chen JZ, Coureux PD, Stroupe ME, Fandrich M, Grigorieff N. High-resolution electron microscopy of helical specimens: a fresh look at tobacco mosaic virus. J Mol Biol. 2007;371(3):812–35. https://doi.org/10.1016/j.jmb.2007.05.088.
37. Wang YH, Hou AJ, Chen L, Chen DF, Sun HD, Zhao QS, Bastow KF, Nakanish Y, Wang XH, Lee KH. New isoprenylated flavones, artochamins A-E, and cytotoxic principles from *Artocarpus chama*. J Nat Prod. 2004;67:757–61. https://doi.org/10.1021/np030467y.
38. Sasaki H, Kashiwada Y, Shibatav H, Takaishi Y. Prenylated flavonoids from the roots of *Desmodium caudatum* and evaluation of their antifungal activity. Planta Med. 2012;78(17):1851–6. https://doi.org/10.1055/s-0032-1315391.
39. Yin S, Fan CQ, Wang Y, Dong L, Yue JM. Antibacterial prenylflavone derivatives from *Psoralea corylifolia*, and their structure-activity relationship study. Bioorg Med Chem. 2004;12(16):4387–92. https://doi.org/10.1016/j.bmc.2004.06.014.
40. Syah YM, Juliawaty LD, Achmad SA, Hakim EH, Ghisalberti EL. Cytotoxic prenylated flavones from *Artocarpus champeden*. J Nat Med. 2006;60:308–12. https://doi.org/10.1007/s11418-006-0012-z.
41. Gabriele B, Salerno G, Fazio A, Veltri L. Versatile synthesis of pyrrole-2-acetic esters and (pyridine-2-one)-3-acetic amides by palladium-catalyzed, carbon dioxide-promoted oxidative carbonylation of (*Z*)-(2-en-4-ynyl) amines. Adv Synth Catal. 2006;348(15):2212–22. https://doi.org/10.1002/adsc.200606085.
42. Huang WB, Chen SM, Chen ZY, Yue MI, Li MH, Gu YL. Synthesis of multisubstituted pyrroles from enolizable aldehydes and primary amines promoted by iodine. J Org Chem. 2019;84(9):5655–66. https://doi.org/10.1021/acs.joc.9b00596.
43. Li YK, Zhao YL, Xiang NJ, Yang L, Wang F, Yang GY, Wang ZY. Flavonoids from the leaves of *Nicotiana tabacum* and their anti-tobacco mosaic virus activity. Heterocycles. 2014;89(12):2771–6. https://doi.org/10.3987/com-14-13108.

44. Zheng CP, Xiong W, Zhang LF, Jin W, Zhang JD, Li YK, Hu QF, Min Z, Kong GH, Ye YQ, Wu YP. Two new anti-tobacco mosaic virus quinolin-2(1*H*)-ones from the twigs of *Cassia auriculata*. Chem Nat Compd. 2023;59(1):107–10. https://doi.org/10.1007/s10600-023-03928-6.
45. Liu HY, Yang FX, Liang MJ, Liu X, Li XM, Kong WS, Mi QL, Guo YD, Yang GY, Deng L, Zhang JD. Two new furo[3,2-*c*]quinolines from the stems of *Nicotiana tabacum* and their anti-tobacco mosaic virus activity. Chem Nat Compd. 2022;58(4):708–11. https://doi.org/10.1007/s10600-022-03773-z.
46. Jiang JR, Zhang JD, Yin GY, Shi JQ, Cai BB, Yang WW, Deng LL, Xu L, Zhou T, Hu QF, Zhou M, Kong WS. Chromone derivatives from *Cassia auriculata* and their antibacterial activity. Chem Nat Compd. 2022;58(3):420–3. https://doi.org/10.1007/s10600-022-03698-7.
47. Ferreyra MLF, Rius SP, Casati P. Flavonoids: biosynthesis, biological functions, and biotechnological applications. Front Plant Sci. 2012;3:222. https://doi.org/10.3389/fpls.2012.00222.
48. Pei TL, Yan MX, Huang YB, Wei YK, Martin C, Zhao Q. Specific flavonoids and their biosynthetic pathway in *Scutellaria baicalensis*. Front Plant Sci. 2022;13:866282. https://doi.org/10.3389/fpls.2022.866282.
49. Yamamoto H, Zhao P, Inoue K. Origin of two isoprenoid units in a lavandulyl moiety of sophoraflavanone G from sophora flavescens cultured cells. Phytochemistry. 2002;60(3):263–7. https://doi.org/10.1016/S0031-9422(02)00111-5.
50. Xu WJ, Xu XY, Han R, Wang XL, Wang K, Qi G, Ma PT, Komatsuda T, Liu C. Integrated transcriptome and metabolome analysis reveals that flavonoids function in wheat resistance to powdery mildew. Front Plant Sci. 2023;14:1125194. https://doi.org/10.3389/fpls.2023.1125194.
51. Bajpai S, Shukla PS, Asiedu S, Pruski K, Prithiviraj B. A biostimulant preparation of brown seaweed ascophyllum nodosum suppresses powdery mildew of strawberry. Plant Pathol J. 2019;35:406–16. https://doi.org/10.5423/PPJ.OA.03.2019.0066.
52. Cole JS. Powdery mildew of tobacco. In: Spencer DM, editor. The powdery mildews. London: Academic Press; 1978. p. 447–67.
53. Pathak R, Ergon A, Stensvand A, Gislerod HR, Solhaug KA, Cadle-Davidson L, Suthaparan A. Functional characterization of pseudoidium neolycopersici photolyase reveals mechanisms behind the efficacy of nighttime uv on powdery mildew suppression. Front Microbiol. 2020;11:1091. https://doi.org/10.3389/fmicb.2020.01091.
54. Obydennov K, Kalinina TA, Galieva NA, Beryozkina TV, Zhang Y, Fan ZJ, Glukhareva TV, Bakulev VA. Synthesis, fungicidal activity, and molecular docking of 2-acylamino and 2-thioacylamino derivatives of 1*H*-benzo[*d*]imidazoles as anti-tubulin agents. J Agric Food Chem. 2021;69(40):12048–62. https://doi.org/10.1021/acs.jafc.1c03325.
55. Manikandan A, Parthasarathy R, Anusuya S, Huang JY. An overview of plant defense-related enzymes responses to biotic stresses. Plant Gene. 2021;27(4):100302. https://doi.org/10.1016/j.plgene.2021.100302.
56. Liu B, Stevens-Green R, Johal D, Buchanan R, Geddes-Mcalister J. Fungal pathogens of cereal crops: proteomic insights into fungal pathogenesis, host defense, and resistance. J Plant Physiol. 2022;269:153593. https://doi.org/10.1016/j.jplph.2021.153593.
57. Hou SJ, Kenichi T. Salicylic acid and jasmonic acid crosstalk in plant immunity. Essays Biochem. 2022;66(5):647–56. https://doi.org/10.1042/EBC20210090.
58. Halim VA, Vess A, Scheel D, Rosahl S. The role of salicylic acid and jasmonic acid in pathogen defence. Plant Biol (Stuttg). 2006;8(3):307–13. https://doi.org/10.1055/s-2006-924025.
59. Chen DM, Li ZM, Huang CY, Yang HJ. Self-digestive solution of Lysobacter enzymogenes LE16 as a biofungicide to control plant powdery mildew. Arch Agron Soil Sci. 2023;69:1–13. https://doi.org/10.1080/03650340.2023.2180799.
60. Irieda H, Takano Y. Epidermal chloroplasts are defense-related motile organelles equipped with plant immune components. Nat Commun. 2021;12(1):2739. https://doi.org/10.1038/s41467-021-22977-5.
61. Zhao TL, Yao RM, Wang W, Zhang YJ, Li CH, Li Y. Genome-wide identification and characterisation of phenylalanine ammonia-lyase gene family in grapevine. J Hortic Sci Biotech. 2021;96(4):456–68. https://doi.org/10.1080/14620316.2021.1879685.
62. Vega K, Kalkum M. Chitin, chitinase responses, and invasive fungal infections. Int J Microbiol. 2012;2012:920459. https://doi.org/10.1155/2012/920459.
63. Breen S, Williams SJ, Outram M, Kobe B, Solomon PS. Emerging insights into the functions of pathogenesis-related protein 1. Trends Plant Sci. 2017;22(10):871–9. https://doi.org/10.1016/j.tplants.2017.06.013.

Publisher's Note